

# UCLA

## UCLA Previously Published Works

### Title

Life on the edge: active microbial communities in the Kryos MgCl<sub>2</sub>-brine basin at very low water activity

### Permalink

<https://escholarship.org/uc/item/5p2856v5>

### Journal

The ISME Journal: Multidisciplinary Journal of Microbial Ecology, 12(6)

### ISSN

1751-7362

### Authors

Steinle, Lea  
Knittel, Katrin  
Felber, Nicole  
[et al.](#)

### Publication Date

2018-06-01

### DOI

10.1038/s41396-018-0107-z

Peer reviewed



# Life on the edge: active microbial communities in the Kryos MgCl<sub>2</sub>-brine basin at very low water activity

Lea Steinle <sup>1,2</sup> · Katrin Knittel<sup>3</sup> · Nicole Felber<sup>1</sup> · Claudia Casalino<sup>4</sup> · Gert de Lange<sup>4</sup> · Chiara Tessarolo<sup>5</sup> · Alina Stadnitskaia<sup>6</sup> · Jaap S. Sinninghe Damsté<sup>4,6</sup> · Jakob Zopf <sup>1</sup> · Moritz F. Lehmann <sup>1</sup> · Tina Treude<sup>7,8</sup> · Helge Niemann<sup>1,6,9</sup>

Received: 22 September 2017 / Revised: 19 January 2018 / Accepted: 12 March 2018 / Published online: 17 April 2018  
© International Society for Microbial Ecology 2018

## Abstract

The Kryos Basin is a deep-sea hypersaline anoxic basin (DHAB) located in the Eastern Mediterranean Sea (34.98°N 22.04°E). It is filled with brine of re-dissolved Messinian evaporites and is nearly saturated with MgCl<sub>2</sub>-equivalents, which makes this habitat extremely challenging for life. The strong density difference between the anoxic brine and the overlying oxic Mediterranean seawater impedes mixing, giving rise to a narrow chemocline. Here, we investigate the microbial community structure and activities across the seawater–brine interface using a combined biogeochemical, next-generation sequencing, and lipid biomarker approach. Within the interface, we detected fatty acids that were distinctly <sup>13</sup>C-enriched when compared to other fatty acids. These likely originated from sulfide-oxidizing bacteria that fix carbon via the reverse tricarboxylic acid cycle. In the lower part of the interface, we also measured elevated rates of methane oxidation, probably mediated by aerobic methanotrophs under micro-oxic conditions. Sulfate reduction rates increased across the interface and were highest within the brine, providing first evidence that sulfate reducers (likely *Desulfovermiculus* and *Desulfobacula*) thrive in the Kryos Basin at a water activity of only ~0.4 *A<sub>w</sub>*. Our results demonstrate that a highly specialized microbial community in the Kryos Basin has adapted to the poly-extreme conditions of a DHAB with nearly saturated MgCl<sub>2</sub> brine, extending the known environmental range where microbial life can persist.

## Introduction

Environments characterized by salinities higher than 50 PSU are considered hypersaline [1]. Such environments are challenging for life due to the high energetic costs for

osmotic adaptation [2] and the limitation of available water [3]. Despite these constraints, microbial and eukaryotic life has been reported in many of these systems [2, 4]. Hypersaline environments exist in terrestrial settings (e.g., lakes, salt flats, salterns), and marine environment (e.g., mud volcanoes, sea-ice brine channels or brine basins [5]). Furthermore, hypersaline settings were also discovered on extraterrestrial objects, for example on Mars, or on Saturn's moon Enceladus [6–8] (Hsu et al. 2015). Hence,

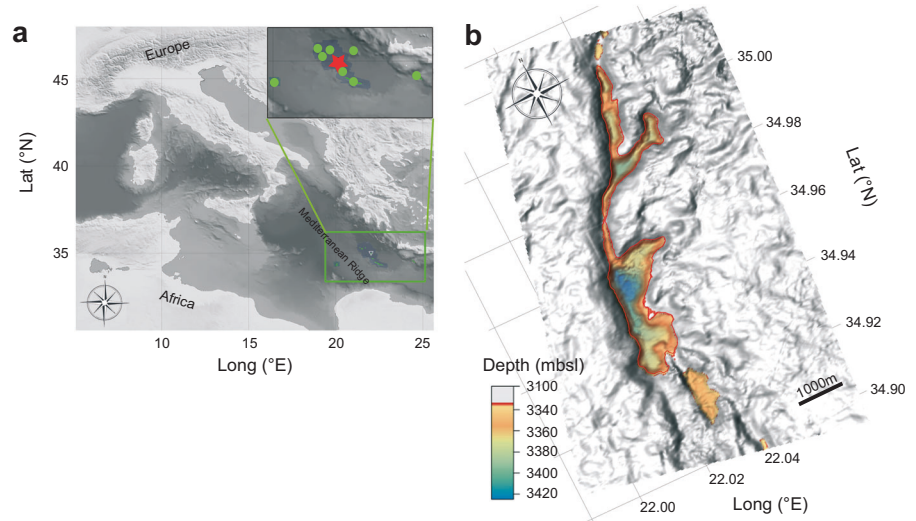
**Electronic supplementary material** The online version of this article (<https://doi.org/10.1038/s41396-018-0107-z>) contains supplementary material, which is available to authorized users.

✉ Lea Steinle  
lea.steinle@unibas.ch

- <sup>1</sup> Department of Environmental Sciences, University of Basel, Basel, Switzerland
- <sup>2</sup> GEOMAR, Helmholtz Centre for Ocean Research, Kiel, Germany
- <sup>3</sup> Max-Planck-Institute for Marine Microbiology, Bremen, Germany
- <sup>4</sup> Department of Earth Sciences, Faculty of Geosciences, Utrecht University, Utrecht, The Netherlands
- <sup>5</sup> Department of Earth and Environmental Sciences, University of Milano-Bicocca, Milan, Italy

- <sup>6</sup> Department of Marine Microbiology and Biogeochemistry, NIOZ Royal Netherlands Institute for Sea Research and Utrecht University, Texel, The Netherlands
- <sup>7</sup> Department of Earth, Planetary and Space Sciences, University of Los Angeles, Los Angeles, CA, USA
- <sup>8</sup> Department of Atmospheric and Oceanic Sciences, University of Los Angeles, Los Angeles, CA, USA
- <sup>9</sup> Department of Geology, Centre for Arctic Gas Hydrate, Environment and Climate, UiT the Arctic University of Norway, 9037 Tromsø Norway

**Fig. 1** **a** Overview map of DHABs in the Eastern Mediterranean. The position of the Kryos Basin is indicated with a red star, the other basins with green dots. **b** Bathymetry of the Kryos Basin and the adjacent seafloor (resolution = 30 m). The extent of the Kryos brine basin is delimited with a dark orange line, and the depth of the basin is indicated by the colored scale bar



hypersaline environments on Earth may serve as analogs for potential niches for life in extraterrestrial environments [9]. Marine brine basins have been discovered at the seafloor of the Gulf of Mexico, the Red Sea, the Black Sea, and the Eastern Mediterranean Sea (see ref. [10], for a review). The deep-sea hypersaline anoxic basins (DHABs) in the Mediterranean are located at the Mediterranean Ridge at water depths >3000 m below sea level (mbsl). Mediterranean brines originate from the dissolution of evaporites deposited during the Messinian salinity crisis (5–6 million years ago [11–13]). After sediment burial, tectonic activity mobilized relic brines and re-exposed some of these evaporite layers to seawater. Their exposure at the seafloor led to the formation of the present-day brine lakes [14–16]. As hypersaline solutions have a higher density than seawater, brines accumulate in seafloor depressions and form lake-like features, which can be several kilometers long and more than hundred meters deep [10, 12]. Even though many DHABs in the Mediterranean are located in close proximity to each other, their respective geochemical composition can differ quite strongly, depending on the source evaporite [10]. The brines of most Mediterranean DHABs (l'Atalante, Bannock, Thetis, Tyro, and Urania basins [17, 18]) are thalassohaline, i.e., the brine salts consist mainly of NaCl. In contrast, the Kryos and the Discovery Basin contain athalassohaline brines, dominated by MgCl<sub>2</sub> [15, 19].

Vertical mixing across the extreme density gradients between brine and overlying seawater is extremely slow. Seawater and brines differ strongly in their solute composition (in particular, in the concentrations of key electron donors and acceptors), so that a narrow (1–3 m) chemocline forms between the two media [10, 20]. In contrast to the overlying seawater, the brines are anoxic but electron acceptors other than oxygen are plentiful, most importantly

sulfate [10]. Hence, hotspots of biological activity were found at brine–seawater interfaces [2, 17, 19, 21–24]. In addition to active microbial communities at the interface, previous studies have provided evidence for microbial activity (sulfate reduction, methanogenesis, and heterotrophy) within thalassohaline brines [17, 18] (Daffonchio et al. 2006). Life in athalassohaline MgCl<sub>2</sub>-rich brines, on the other hand, is considered much more challenging [17, 19, 25]. In fact, microbial life was considered impossible in the Kryos brine basin due to its extremely high concentrations of MgCl<sub>2</sub> [19], and putative evidence for life in the nearby Discovery Basin [17] has been questioned [25, 26]. Major challenges for microbial life in MgCl<sub>2</sub>-brines, in addition to osmotic stress, are chaotropicity (i.e., the disruption of hydrogen bonding network between water molecules causing denaturation of organic molecules [3], Cray et al. 2013) and exceptional low levels of water activity— $A_w$  ( $A_w$ —the vapor pressure of an aqueous solution relative to distilled water).  $A_w$  is a key parameter used to determine the limits of life [27]. It takes thermodynamically available water into account—in contrast to water content (percentage water)—and thus describes water availability on the organismic level due to binding effects promoted by ions [28]. Cell division, for example, has only been observed at  $A_w \geq 0.605$   $A_w$  (Stevenson et al. 2015), much higher than the  $A_w$  of ~0.4 that has been experimentally determined for the Kryos brine [19].

The main objective of this study is to determine whether the poly-extreme environmental conditions (anoxia, hypersalinity, chaotropicity) prevailing in the Kryos brine permit active microbial life. Towards this goal we use an interdisciplinary approach that combines geochemical measurements (i.e., major ions, methane), direct

measurements of microbial activity (sulfate reduction and methane oxidation with radio-tracer assays), as well as lipid biomarker analyses and next-generation sequencing (NGS) of 16S rRNA genes to assess the microbial community structure.

## Methods

### Study site

The Kryos Basin (34.93°N 22.02°E–35.02°N 22.05°E; Fig. 1) is one of eight known DHABs located in the Eastern Mediterranean Sea [10, 19] (Fig. 1), and is filled with brine originating from secondary late-stage evaporites, dominated by  $\text{MgCl}_2$ . Its composition is similar to that of the Discovery brine [15, 29], but with even higher concentrations of  $\text{Na}^+$  and  $\text{SO}_4^{2-}$  [19]. Samples presented in this study were collected on the “Ristretto e Lungo” Cruise (2010/2011) with the RV Meteor (Me83/3) within the framework of the “Moccha” and “Middle” projects (Eurodeep-Program of the European Science Foundation).

### Sampling

Water samples were collected in January 2012 from the deepest part of the Kryos Basin (34.952°N 22.025°E; Fig. 1) using a rosette sampler equipped with 12 × 10 L Niskin bottles and probes for continuous measurements of conductivity, temperature and density (CTD; Seabird SBE9). We sampled the water column just above the seawater–brine interface, within the interface, and in the brine. The position of the interface was detected with the conductivity sensor (mounted at the lower part of the rosette sampler frame) in real-time during the hydrocast [22]. For interface sampling, several Niskin bottles were closed in quick succession immediately after a conductivity increase was detected, while slowly lowering the sampler through the interface [20]. This way, each bottle contained sea-/brine water collected at slightly different depths within the interface (Fig. 2). During recovery, the strong density gradient prevented vertical mixing within the bottle, preserving the in situ stratified conditions [22]. Upon retrieval, each bottle was sampled successively (at ~2 l batches, yielding a vertical resolution of ~20 cm). Distinct sampling within each batch was done following the same sequence: first for volatiles ( $\text{CH}_4$ ,  $\text{HS}^-$ ), dissolved  $\text{O}_2$  and DIC, then for microbial rate measurements, and finally for the analysis of major elements, nutrients, and  $\text{SO}_4^{2-}$ . See supplements for details on standard geochemical analyses. The relative positions of the different Niskin bottles (Fig. 2) were aligned using

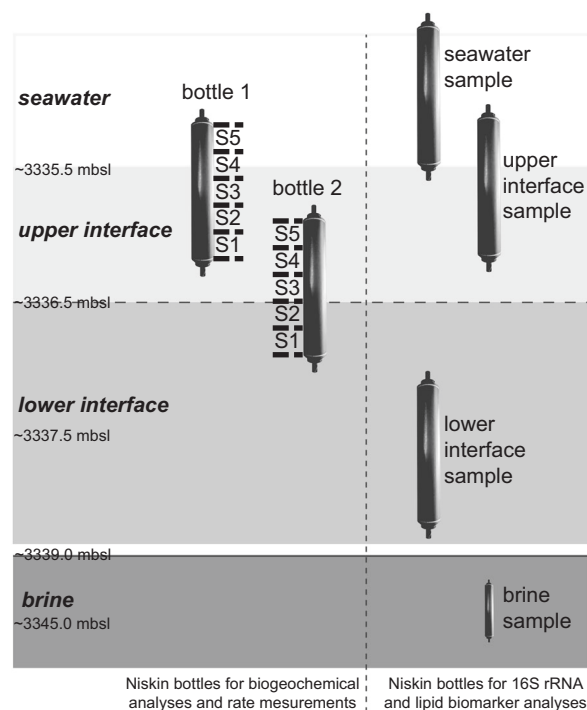


**Fig. 2** Scheme for high-resolution sampling across the seawater–brine interface with Niskin Bottles. Interface sampling was conducted during very calm weather conditions with minimal pitch/roll of the ship, preventing erratic up and down movement of the water sampler. The strong density difference impeded mixing of seawater and brine in the closed Niskin bottles during recovery. Immediately upon recovery, each Niskin bottle was sampled repeatedly (5–7 cycles) for different parameters resulting in a vertical resolution of the water column of ~20 cm. Vertical depth profiles were aligned based on chlorinity. Separate bottles were taken for 16S rRNA and biomarker analyses

$\text{Cl}^-$  concentrations as a conservative tracer, as described previously [19]. Separate Niskin bottles were taken for lipid biomarker and NGS analyses, just above the interface ( $3335.0 \pm 0.5$  mbsl), in the upper ( $3335.8 \pm 0.5$  mbsl) and lower ( $3337.8 \pm 0.5$  mbsl) interface, and in the brine ( $3344.6 \pm 1$  mbsl; Fig. 2).

### Methane oxidation and sulfate reduction rate measurements

Water samples for methane oxidation and sulfate reduction (SR) rate measurements were filled bubble-free into 20 mL glass vials, closed with bromobutyl stoppers [30] and incubated in quadruplicates with  $^{14}\text{C}$  and  $^{35}\text{S}$  radiotracers, respectively, for 72 h at in situ T in the dark [31, 32]. Incubations were terminated, and samples fixed and stored, as described in Steinle et al. [33]. For SR rates, one teaspoon of kaolin powder was added to samples to facilitate separation of  $\text{SO}_4^{2-}$  and  $\text{ZnS}$ , and SR rates were then determined with the cold-chromium distillation method [34]. MOx rates and the fraction of methane incorporated into biomass were assessed as described previously [35, 36].

**Table 1** Geochemical parameters and rate measurements within the Kryos brine basin and across the seawater–brine interface

	Brine	Lower interface		Upper interface		Seawater
Depth (mbsl)	>3344	3337	3336.5	3336.4	3335.7	3335.6
Cl <sup>-</sup> (mmol kg <sup>-1</sup> )	6545	1421	1200	1055	606	594
Na <sup>+</sup> (mmol kg <sup>-1</sup> )	75	366	428	483	510	510
Mg <sup>2+</sup> (mmol kg <sup>-1</sup> )	3936	665	466	221	83	67
SO <sub>4</sub> <sup>2-</sup> (mmol kg <sup>-1</sup> )	144.2	61	52	40	31	30
O <sub>2</sub> (μmol kg <sup>-1</sup> )	ns	0	0	3	182	193
NH <sub>4</sub> (μmol kg <sup>-1</sup> )	940	137	83	73	2	1.5
HS <sup>-</sup> (μmol kg <sup>-1</sup> )	150	64	0	0.8	0	0
CH <sub>4</sub> (μmol kg <sup>-1</sup> )	20	11	2	4	0.2	0
C <sub>2+</sub> (μmol kg <sup>-1</sup> )	1.25	bd	bd	bd	bd	bd
DIC (μmol kg <sup>-1</sup> )	4150	4060	3704	3747	2517	2445
δ <sup>13</sup> C-DIC (‰)	-0.1	-0.8	0.6	0.7	0.8	ns
δ <sup>13</sup> C-CH <sub>4</sub> (‰)	-47.1	-41.9	-43.2	-45.7	ns	ns
δD-CH <sub>4</sub> (‰)	-128.9	-122.1	-109.5	ns	ns	ns
MOx rate (nmol kg <sup>-1</sup> d <sup>-1</sup> )	1.2 ± 1.9	58 ± 12	7.2 ± 0.8	8.0 ± 7.7	0.13 ± 0.04	ns
SR rate (μmol kg <sup>-1</sup> d <sup>-1</sup> )	457 ± 346	16 ± 2	5.7 ± 1.4	9.8	1.8 ± 1.7	ns

For the upper and lower interface, the value on the left represents the value for the deepest sample, the value on the right the value for the shallowest sample. For rates of methane oxidation (MOx) and sulfate reduction (SR) standard deviation is indicated, if applicable

ns not sampled, bd below detection, C<sub>2+</sub> hydrocarbons with two and more carbon atoms

All rate measurements were corrected for abiotic tracer turnover (<1% of live controls) in killed controls using the same matrix (i.e., seawater, interface water, or brine). We considered only rates that were at least as high as the mean tracer turnover in killed controls plus three standard deviations of the killed-control value [37].

### Biomarker analyses

For lipid biomarker analyses, 20 L of water/brine (combined from 2–3 Niskin bottles) from each layer (seawater, upper and lower interface, brine) was filtered on glass microfiber filters (GF/F, particle retention ~0.7 μm), and stored at -80 °C until extraction in the home laboratory. The largest portion (7/8th) of each filter (corresponding to ~17.5 L water/brine) was used for lipid extraction according to Elvert et al. [38], but we added an additional extraction step with methanol:H<sub>2</sub>O (1:3; v/v) to extract polar compounds. The resulting total lipid extract was further separated and analyzed according to Elvert et al. [38] and Niemann et al. [39]. Double-bond positions of monoenoic fatty acids were determined by analyzing fatty-acid dimethyl disulfide derivatives [40, 41]. Identities, concentrations, and stable carbon isotope composition of individual compounds were determined with a gas chromatograph linked either to a quadrupole mass spectrometer, a flame-ionization detector, or an isotope ratio mass spectrometer [36].

### Nucleic acid extraction and amplification of 16S rRNA genes

Nucleic acids were extracted from the remaining 1/8th of a GF/F filter (corresponding to 2.5 L water/brine) according to the method described by Zhou et al. (1996). Prior to extraction, cells were removed from the filters by washing [42] with 5 M NaCl to avoid DNA loss by binding to the glass fiber filters during the extraction process.

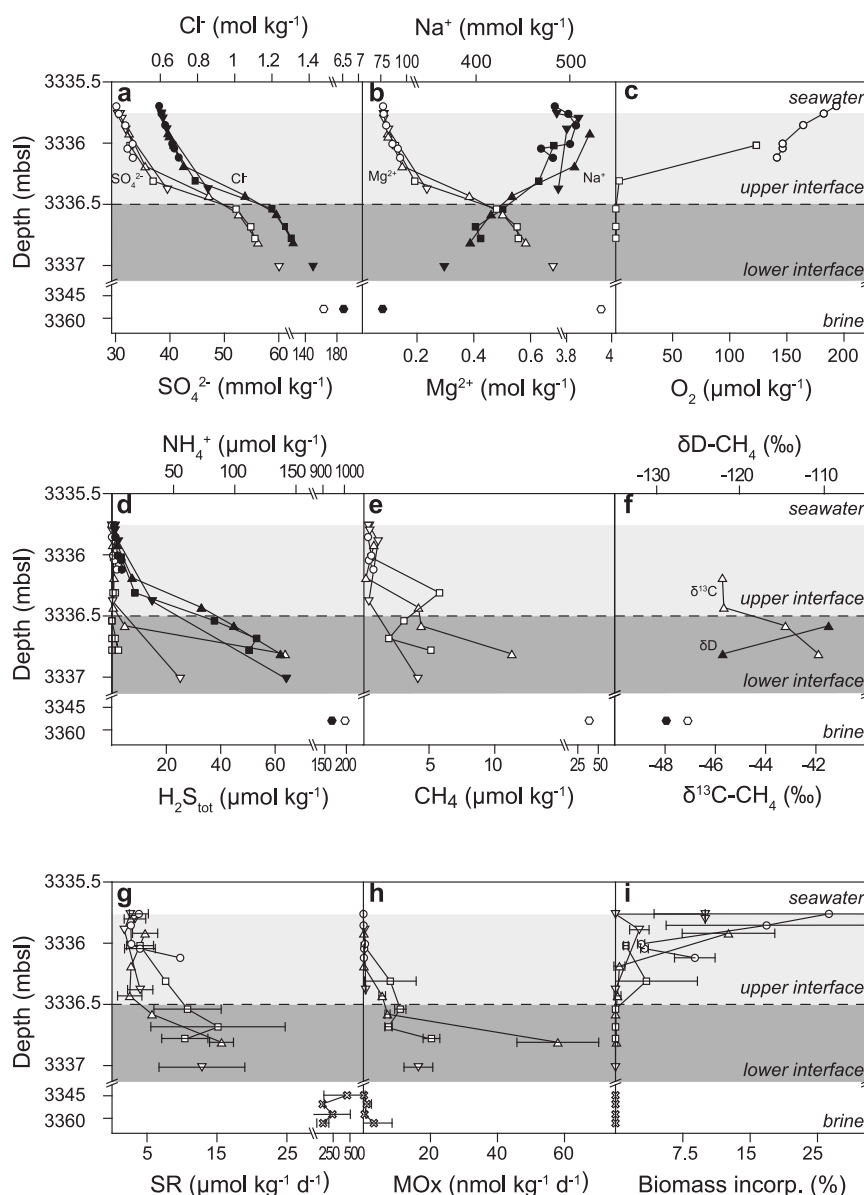
Bacterial 16S rRNA genes were amplified by PCR from extracted DNA using the primer pair Bakt\_341F/Bakt\_785R [43] (Supplementary Table 1). Archaeal 16S rRNA genes were amplified using primer pair ARCH340F/ARCH1000R [44] (Supplementary Table 1). To allow the coverage of ANME-1 methanotrophic archaea and *Korarchaeota*, we added modified primers: ARCH340F-ANME-1, ARCH1000R-ANME-1, and ARCH1000R-KOR (Supplementary Table 1). Forward primers ARCH340F and ARCH340F-ANME-1 were mixed in a molar ratio of 4:1; reverse primers ARCH1000R, ARCH1000R-ANME-1, and ARCH1000R-KOR were mixed in a molar ratio of 8:1:1.

PCR reactions (20 μL volume) were performed using TaKaRa Taq polymerase (Germany) according to Supplementary Table 2. The resulting bacterial 450 bp-amplicons and archaeal 700 bp-amplicons were extracted from an agarose gel (1% w/v) and purified using the MinElute PCR Purification Kit (Qiagen) according to the manufacturer's recommendations.

**Fig. 3** Geochemical profiles and rate measurements across the seawater–brine interface.

Concentrations of **a** chloride (filled symbols) and sulfate (open symbols), **b** magnesium (filled symbols) and sodium (open symbols), **c** oxygen, **d** ammonium (filled symbols) and sulfide (open symbols), **e** methane, and **f** isotopic composition of methane  $-\delta D$  (filled symbols) and  $\delta^{13}C$  (open symbols). Rates of **g** sulfate reduction (SR), and **h** methane oxidation (MOx). **i** Fraction of oxidized methane-C incorporated into biomass.

Values in **a–f** represent single measurements. Error bars in **g–i** represent standard deviations of quadruplicates. The dashed horizontal line indicates the border between upper and lower interface, and the continuous horizontal line the beginning of the brine. Note the different depth scales for the interface and brine. We vertically resolved the interface with four, substantially overlapping Niskin bottle samplings (represented by different symbols: circle, square, upward-, and downward triangle). The profiles from these bottles were aligned based on chlorinity



## Sequencing, sequence processing, and taxonomic analysis

Amplicons were analyzed by massive parallel tag sequencing on a HiSeq 2500 sequencer (2 × 250 bp; Illumina, San Diego, CA) at the Max Planck-Genome-Centre Cologne, Germany. Bacterial reads were quality-trimmed (trimq = 22, minlength = 238, homopolymers ≤ 8 nt) and merged (overlap > 25) using the software package BBmap v4.3, and split using mothur v1.33.3 [45]. Archaeal forward and reverse reads were analyzed separately because amplicons were too long to obtain an overlap of reads. Data shown here are based on reverse reads. Settings for trimming of archaeal sequences were trimq = 25, homopolymers ≤ 8 nt. Archaeal and bacterial sequences were classified using the SILVA pipeline and database release

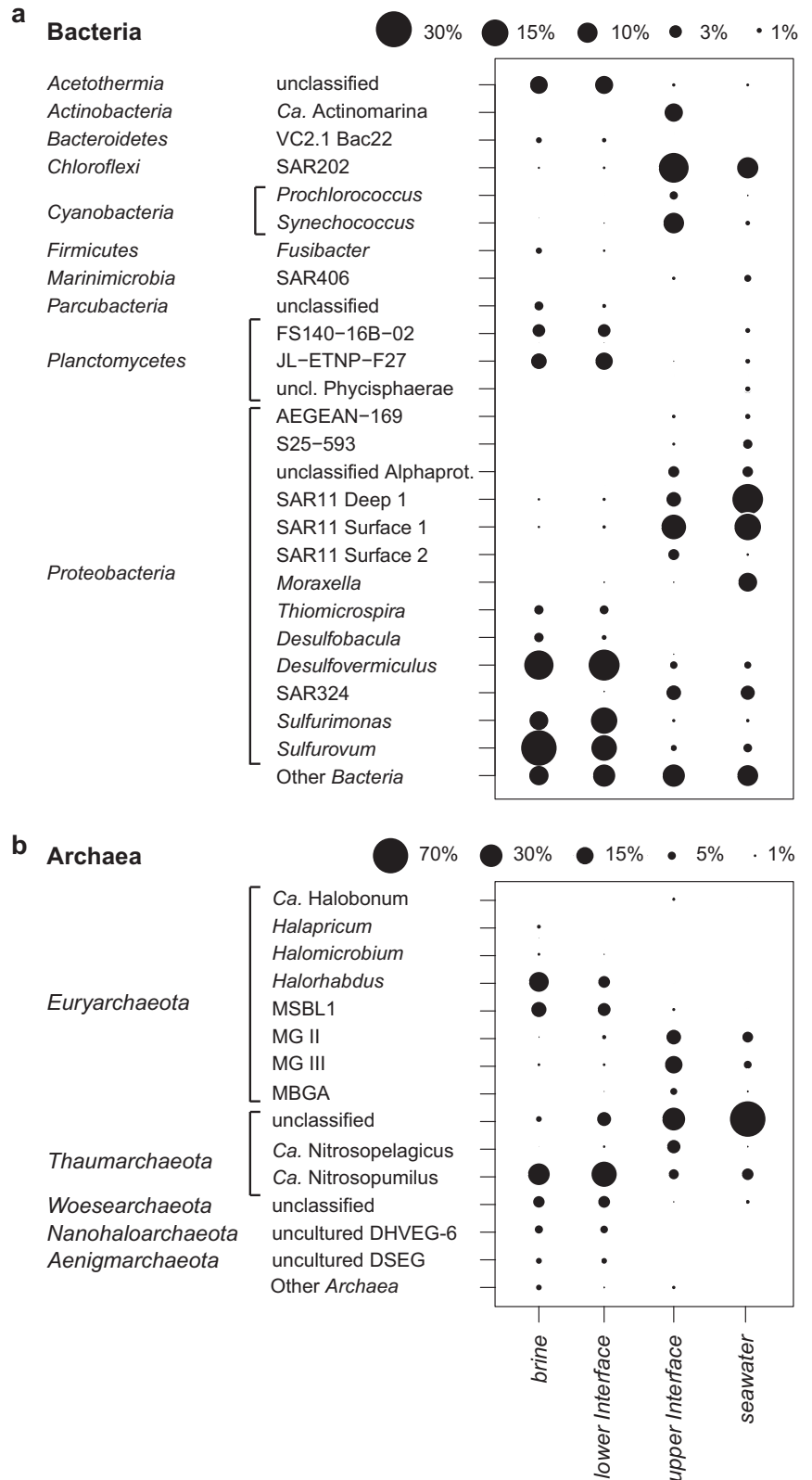
123.1, 03-2016 [46]. Retrieved non-16S rRNA-gene sequences were removed from the analysis. Similarly, from the bacterial sequence dataset, retrieved archaeal sequences were excluded, as they were unspecifically amplified during PCR. Raw reads were deposited at the EBI Short Read Archive (SRA), and can be accessed under the study accession number PRJEB24471.

## Results and discussion

### Chemical stratification across the seawater–brine interface

The Kryos Basin is filled with athallassohaline brine, dominated by MgCl<sub>2</sub> equivalents at near-saturation, and

**Fig. 4** Relative abundances of bacterial and archaeal genera and unclassified clades in the Kryos brine and interface based on sequencing of 16S RNA genes (V3–V4 region for *Bacteria*, V3–V6 region for *Archaea*). Taxonomy is based on SILVAngs, release 123.1. Sequence abundances are given in per cent of total classified *Bacteria* and *Archaea*, respectively. Only taxa that made up >1% of total archaeal or bacterial sequences in any given sample are shown. Archaeal sequence abundances shown in this figure are based on unassembled reverse sequence reads. Forward reads showed a nearly congruent community composition



with strongly elevated SO<sub>4</sub><sup>2-</sup>-levels (~5-fold seawater concentration; Table 1). Accounting for MgCl<sub>2</sub> and MgSO<sub>4</sub> concentrations, density (1.31 kg dm<sup>-3</sup>) and total dissolved

solids (0.46 kg dm<sup>-3</sup>), we calculated a water activity of 0.44 A<sub>w</sub> combining the Pitzer and Samapundo models (according to models by Pitzer [47] and Samapundo et al. [48]). This

stands in relatively good agreement with a more realistic, direct measurement of an  $A_w$ -value of 0.4 for the Kryos brine, which was determined experimentally [19]. Concentrations of  $\text{SO}_4^{2-}$ ,  $\text{Cl}^-$ , and  $\text{Mg}^{2+}$  increased sharply from seawater background values through the interface into the brine, to 0.144, 6.55, and 3.94 mol kg<sup>-1</sup>, respectively (Fig. 3a, b; Table 1), whereas  $\text{Na}^+$  concentrations decreased from 0.510 to 0.075 mol kg<sup>-1</sup> (Fig. 3b; Table 1).

Concentrations of the microbially relevant electron donors  $\text{CH}_4$  and  $\text{H}_2\text{S}_{\text{tot}}$  were low, or below detection limit, in the upper part of the interface, but the concentration of both species increased sharply in the lower interface to maximum concentrations of 20 and 150  $\mu\text{mol kg}^{-1}$ , respectively (Fig. 3c, d; Table 1). In contrast,  $\text{O}_2$  abruptly decreased to values below the detection limit ( $\sim 1 \mu\text{M}$ ) in the lower interface (Fig. 3d). In the following, based on conductivity gradients and  $\text{O}_2$  concentration levels, we will refer to the upper interface as the depth layer between 3335.75 and 3336.5 mbsl, where  $\text{O}_2$  was still detectable (3–193  $\mu\text{mol kg}^{-1}$ ), and no  $\text{H}_2\text{S}_{\text{tot}}$  was measured. The lower interface refers to the depth layer between 3336.5 and 3337.5 mbsl, where  $\text{O}_2$  concentrations were below the detection limit ( $< 1 \mu\text{M}$ ) and increasing levels of  $\text{H}_2\text{S}_{\text{tot}}$  (0–64  $\mu\text{mol kg}^{-1}$ ) were observed. The uppermost samples (3335.5–3335.75; Fig. 3) represent “normal” seawater.

### Stratification of microbial communities

NGS analyses revealed distinct microbial communities in the seawater and the upper interface on the one hand, and within the lower interface and in brine samples on the other hand (Fig. 4). In the seawater end-member above the interface, most sequences were affiliated with typical archaeal and bacterial planktonic groups, i.e., mostly *Thaumarchaeota*, *MG II*, *MG III*, *SAR202*, *SAR11*, and *Moraxella* (Fig. 4). The bacterial and archaeal community composition of the upper interface was comparable to that of the seawater but low abundances of sequences of halophilic archaea were already present (e.g., MSBL1—Mediterranean Sea Brine Lakes 1 and Ca. Halobionum sequences each made up 1% of all classified archaeal sequences). The community composition of the lower interface and the brine comprised a much higher percentage of sequences of known halophilic archaeal groups, such as *Halorhabdus*, *Halomicrobium*, and *Nanohaloarchaeota*, indicating the presence of a halophilic microbial community.

In the lower interface, 13% of the archaeal sequences fell into the candidate division MSBL1, previously found to be one of the key contributors to the halophilic communities in the athalassohaline Discovery brine [17], as well as in most thalassohaline Mediterranean- and Red Sea brine basins

[17, 49, 50] (Yakimov et al. 2013). The most abundant archaeal group both in the lower interface and the brine (49% and 36% of all classified sequences, respectively) was “Ca. Nitrosopumilus”. The presence of these ammonium-oxidizing archaea [51] (Walker et al. 2010), abundant ambient  $\text{NH}_4^+$  and potentially micro-oxic conditions [52, 53] suggests an ammonium-driven nitrogen cycle in the lower interface. In the lower interface and the brine, 9% of all bacterial sequences belonged to the candidate phylum *Acetothermia*, commonly reported from brine environments [17, 22, 49, 54]. This phylum includes previously used but now abandoned candidate divisions Ca. KB1, OP1, and MSBL6. Sequences classified as *Acetothermia* in the lower interface all grouped within the KB1 division, whereas a minor portion of the brine *Acetothermia* sequences ( $\sim 0.2\%$ ) also fell into the group previously classified as MSBL6. Besides these known halophilic/halotolerant bacteria, most other bacterial sequences of the lower interface and the brine were related to sulfate-reducing and sulfur-oxidizing bacteria, as discussed in more detail below. We are aware that DNA of dead organisms may be preserved in anoxic brines, so that 16S rRNA-gene-sequence data can be ambiguous tracers of in situ microbial life at a given depth within the interface and the brines [55, 56] (Orsi et al. 2013). However, we observed a clear “stratification” of the microbial communities in the brine and lower interface, contrasting the upper interface and seawater (Fig. 4), which suggests an organized, and hence living, in situ microbial community. Indeed, most sequences of halophiles found in the lower interface were not present at all or constituted only a minor fraction of the microbial community in the upper interface and the seawater. This precludes that these sequences represent preserved (i.e., non-living) matter from overlying water layers. On the other hand, a small portion of sequences that were most abundant in the seawater and upper interface (e.g., SAR11) were also detected in the lower interface and the brine; these sequences may hence originate from the water layers above. Similarly, the intermixture of dead microbial cells from the lower interface into the brine cannot be ruled out completely (see below).

### Methanotrophy in the interface

The shape of the methane concentration profile across the interface, with abruptly decreasing methane concentrations in the lower interface (Fig. 3e; Supplementary Figure 1a), indicates methane consumption in this water layer. Furthermore,  $\delta^{13}\text{C}$ - and  $\delta\text{D-CH}_4$  values of the lowest interface sample are clearly enriched in  $^{13}\text{C}$  ( $\Delta\delta^{13}\text{C-CH}_{4,\text{interface-brine}} = 5.2\text{‰}$ ) and  $^2\text{H}$  ( $\Delta\delta\text{D-CH}_{4,\text{interface-brine}} = 6.7\text{‰}$ ) compared to methane in the brine (Fig. 3f). This is consistent with methane oxidation occurring in the lower interface as



methanotrophs preferentially use <sup>12</sup>C-methane, and their activity enriches of the remaining methane in both <sup>13</sup>C and <sup>2</sup>H [57]. Indeed, we measured elevated rates of microbial methane oxidation in the upper but also in the lower interface, where sulfide started to accumulate and oxygen concentrations were below detection limit (1–2 μM for Winkler titration; Fig. 3). With specialized sensors, previous studies on methane oxidation at oxic/anoxic interfaces could demonstrate that oxygen is present at sub-micromolar levels even below an “apparent” oxicleine (e.g., [36]). It is thus likely that traces of oxygen were also present in the lower interface at Kryos, serving as potential electron acceptors for methane oxidation besides sulfate. Hence, both aerobic and anaerobic modes of methane oxidation seem thermodynamically feasible. To distinguish between these modes of methane oxidation, supplementary information on the identity of present methanotrophs is needed.

Aerobic oxidation of methane (MOx) is mediated by aerobic methanotrophic bacteria (MOB), which belong to the *Gamma*- (Type I MOB) or *Alphaproteobacteria* (Type II MOB) [58]. In the lower interface, where we also measured highest methane oxidation rates (Fig. 3h), we detected MOB-sequences related to the gammaproteobacterial *Methylococcales* and alphaproteobacterial *Methylobacterium* (although at a relatively low abundance levels of <0.1% of total bacterial sequences; Supplementary Table 3). The presence of MOB within the Kryos interface is also evident from lipid biomarker signatures. Lipids depleted in <sup>13</sup>C relative to the δ<sup>13</sup>C-CH<sub>4</sub> can be diagnostic for MOB in aquatic environments [36, 58–61] (Summons et al. 1994). In the lower interface, we detected diplopterol and diploptene depleted in <sup>13</sup>C (–46.6‰ and –49.6‰, respectively; Supplementary Figure 2). Their δ<sup>13</sup>C-values are ~5‰ lower compared to ambient lower interface methane (–42‰; Fig. 3f). This observation is consistent with previous findings of slightly <sup>13</sup>C-depleted MOB-biomarkers (diploptene, diplopterol) at the oxycline of the Black Sea [60, 62]. We also measured traces of the fatty-acid C16:1ω8, a diagnostic marker for type I MOB. Our DNA and biomarker data strongly suggest that lipids in the suspended particulate matter pool of the interface are partially comprised of MOB biomass, and that methane oxidation rates within the interface at oxygen concentrations below detection limit and highly elevated MgCl<sub>2</sub>-concentrations are mediated by MOB. Several studies targeting oxic/anoxic interfaces in both marine [35, 60, 63] and lacustrine environments [36, 64, 65] reported MOx under micro-oxic conditions, providing evidence that at least some MOB are able to adapt to very low-oxygen conditions, though such conditions may not be optimal for growth [35]. At Kryos, the fraction of oxidized methane-carbon incorporated into biomass decreased from the upper to the lower interface (Fig. 3i).

Similar to findings from hypoxic Baltic Sea waters [35], this suggests that MOB at Kryos live at the very edge of their habitable ecological niche. At the interface of thalassohaline brines, aerobic methanotrophy was already evidenced directly or indirectly [66–68]. With this study, we demonstrate for the first time that MOB can also adapt to micro-oxic conditions in an athalassohaline brine.

Although the environmental conditions within the lower interface would suggest that AOM is more important MOx, we could not find any indications for AOM. AOM with sulfate as the final electron acceptor is mediated by methanotrophic archaea (ANME), which are related to the order *Methanosarcinales* [69]. We did not detect any sequences of ANMEs in the lower interface (Supplementary Table 5), even though we used a primer set specifically modified to target ANME-archaea, and we also did not find any anaerobic methanotrophs using electron acceptors other than sulfate, i.e., nitrite, iron, or manganese [70, 71], (Raghoebarsing et al. 2006; Supplementary Tables 3 and 5). Moreover, our rate measurements did not reveal any methanotrophic activity in the brine itself, despite high levels of methane and sulfate (Fig. 3). Finally, our lipid biomarker analyses did not reveal any typical ANME signatures, such as strongly <sup>13</sup>C-depleted archaeol and crocetane [72]. Although both compounds were present in the lower interface and brine, their δ<sup>13</sup>C-values were relatively high (compared to the isotopic composition of the ambient methane and DIC (Table 1)), which argues against ANMEs as potential source organisms. Conclusively, our results suggest that ANME cannot thrive under the poly-extreme conditions of the Kryos brine [73, 74].

### Methanogenesis in the interface and brine

The isoprenoid lipid archaeol is synthesized by a variety of archaea including methanogens [75]. Crocetane in the marine environment is generally associated with ANMEs [72], but it was also detected in methanogenic sediments suggesting that it is synthesized by at least some methanogens too [76]. Methanogens are hence possible source organisms for the archaeol and crocetane with relatively high δ<sup>13</sup>C-values [77]. Indeed, our microbial diversity analyses provided evidence for the presence of methanogenic archaea within the interface and brine (Supplementary Tables 5 and 6): 0.5% of total archaeal sequences within the brine belonged to methanogenic archaea of the order *Methanosarcinales*, most importantly *Methanohalophilus*. Sporadically, sequences related to other methanogens (*Methanoseta*, *Methanoregula*, *Methermicrococcus*, *Methanobrevibacter*, *Methanoregula*, and *Methanobolus*) were also detected throughout the interface. As indicated by its isotopic composition (δ<sup>13</sup>C = –47.1‰, δD = –128.9‰;

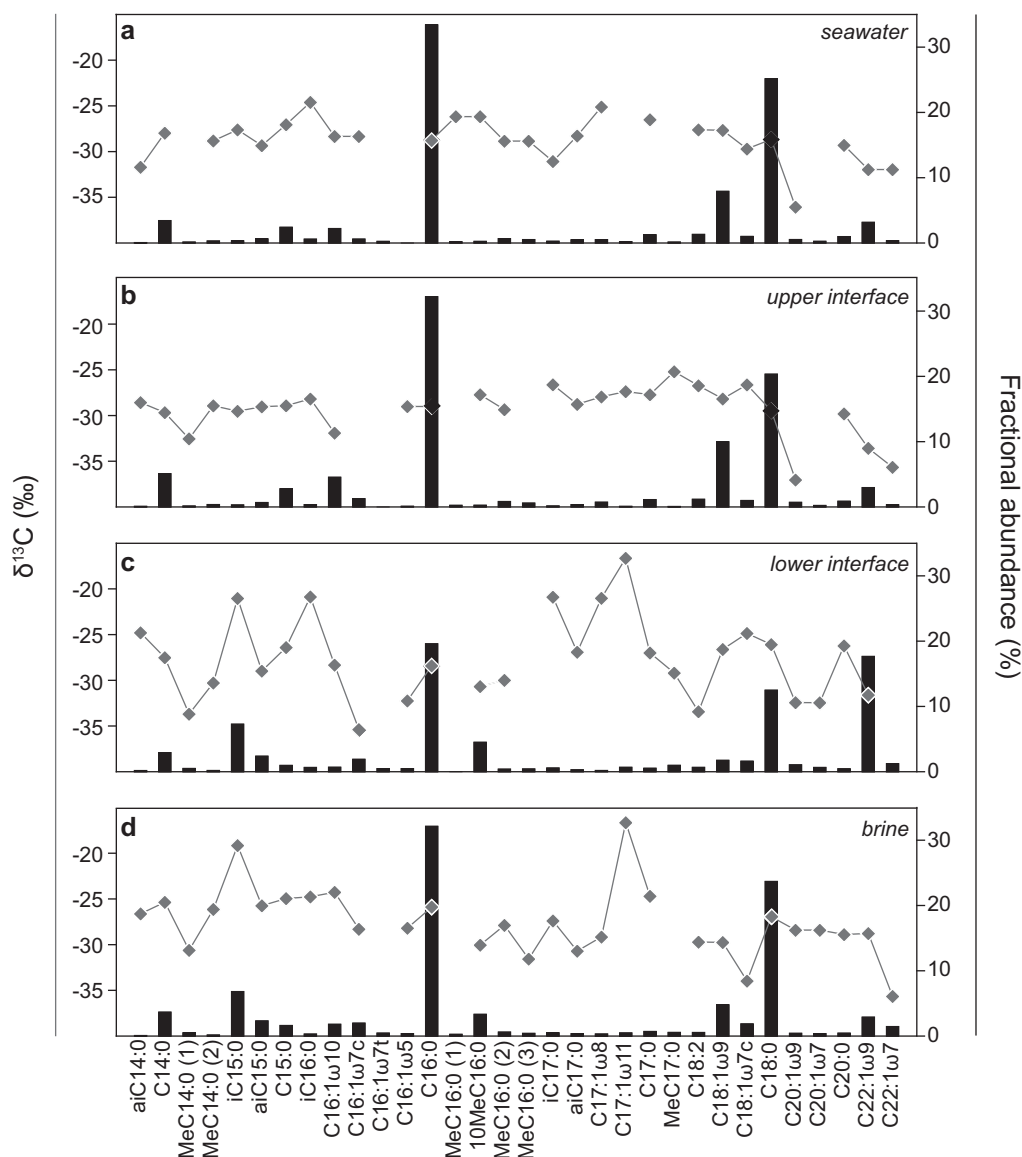


**Fig. 5** Fatty-acid fingerprints across the seawater–brine interface. Fractional abundance (black bars) and compound-specific  $\delta^{13}\text{C}$ -values (diamonds, gray line) of fatty acids (C14–C22) from **a** the seawater, **b** the upper interface, **c** the lower interface, and **d** the brine. The fingerprint comprised fatty acids with methyl groups at the iso (i) or anteiso (ai) position, or at carbon atom position 10 (10 Me). In several cases, we could not determine the position of the methyl branch in the

alkyl chain. Chain isomerism was then denoted by sequential numbers in parentheses (e.g., MeC14:0(1) and MeC14:0(2)). Mass traces of C16:1 $\omega$ 8 were detected as DMDs-derivate in interface and brine samples. Concentration-weighted averages of bulk fatty-acid  $\delta^{13}\text{C}$ -values are  $-28.9\text{‰}$  (seawater),  $-29\text{‰}$  (upper interface),  $-28.6\text{‰}$  (lower interface),  $-26.6\text{‰}$  (brine)

[57]) and its ratio relative to higher hydrocarbons ( $\text{CH}_4:\text{C}_{2+} = 24$ ; [78]), methane in the Kryos Basin is dominantly of thermogenic origin. Yet, the admixture of biogenic methane is likely. The vertical profile of methane  $\delta^{13}\text{C}$ -values across the interface shows  $^{12}\text{C}$ -enriched methane in the upper interface when compared to the lower interface (Fig. 3f). This observation cannot be explained by simple mixing with the overlying seawater, but indicates input of microbial methane within the upper interface [57]. We found *Methanohalophilus* in the upper interface, but whether these methanogenic archaea are the source

of the apparent methane input and can tolerate the oxic conditions prevailing in the upper interface remains questionable.

### Sulfide oxidation within the interface: biomarker and molecular indication for thiotrophs potentially using the rTCA pathway for $\text{CO}_2$ fixation

Sulfide concentrations, similar to methane concentrations, sharply decreased to values below the detection limit at the boundary between the upper and lower interface, indicating

sulfide consumption mainly in the lower interface (Supplementary Figure 1b). Sulfide oxidation is mediated by a diversity of bacterial groups, typically by members of the Gamma- and Epsilonproteobacteria (e.g., [23, 24, 49, 79]). Indeed, we found abundant sequences related to sulfide-oxidizing Epsilonproteobacteria in the lower interface and in the brine: *Sulfurimonas*- and *Sulfurovum*-related sequences accounted for 16% and 15%, respectively, of the total bacterial sequences in the lower interface, and 8% and 29%, respectively, in the brine (Fig. 4). Moreover, gammaproteobacterial *Thiomicrospira*-related sequences constituted ~3% of all bacterial sequences both in the lower interface and the brine (Fig. 4). In contrast, the abundance of these thiotrophs in the upper interface and the seawater was very low ( $\ll 1\%$ ). Yakimov et al. [19] also detected one sequence of the *Sulfurovum* clade in the lower interface of the Kryos Brine, but did not find molecular evidence for *Sulfurimonas*. Similarly, thiotrophs are important parts of the microbial communities at other seawater–brine interfaces in the Mediterranean (e.g., Thetis brine: [24], Urania brine: [49], L'Atalante brine: [23]).

Within the lower interface and the brine, our lipid analysis revealed several fatty acids that were enriched in <sup>13</sup>C (with  $\delta^{13}\text{C}$ -values up to  $-18\%$ ; Fig. 5) compared to the other fatty acids (concentration-weighted average:  $-28.6\%$ —lower interface,  $-26.6\%$ —brine). Similar to our findings, biomass at hydrothermal vents partitions into two isotopically distinct clusters (see ref. [79], for a review). The more strongly <sup>13</sup>C-depleted values were explained by the large C-isotope fractionation during carbon fixation via the Calvin–Benson cycle [79], which is characterized by a C-isotope enrichment factor ( $\Delta\delta^{13}\text{C}_{\text{CO}_2\text{-biomass}}$ ) of  $20\%$ – $30\%$  [80]. This is the most common carbon fixation pathway in the bacterial realm. In contrast, the more <sup>13</sup>C-enriched signatures often originate from other carbon fixation pathways, such as the reductive tricarboxylic acid cycle (rTCA), which is characterized by a comparatively low  $\Delta\delta^{13}\text{C}$  of only  $2\%$ – $12\%$  [77, 80]. Because of the isotopic fractionation between CO<sub>2</sub> and DIC [81], CO<sub>2</sub> at Kryos is probably more depleted than DIC ( $\delta^{13}\text{C}$ -DIC:  $-0.8\%$  to  $0.8\%$ ). Together with  $\delta^{13}\text{C}$ -values of the fatty acids of about  $-18\%$ , the  $\Delta\delta^{13}\text{C}_{\text{CO}_2\text{-fatty acids}}$  would thus be  $\ll 18\%$ . Considering additional C-isotope fractionation during fatty-acid synthesis of  $\sim 2\%$ – $10\%$  [82–84], the <sup>13</sup>C-enriched fatty acids may indeed originate from organisms utilizing the rTCA cycle. Some of the <sup>13</sup>C-enriched fatty acids (iC15:0, iC16:0 and iC17:0) are of bacterial origin [85, 86], but are not diagnostic for any specific phylogenetic group. The source organisms of the other two <sup>13</sup>C-enriched fatty acids (17:1 $\omega$ 8 and 17:1 $\omega$ 11) remain unknown. Nevertheless, we suggest that the epsilonproteobacterial sulfide-oxidizers detected at Kryos

(Fig. 4) are the source organisms of the <sup>13</sup>C-enriched fatty acids, likely fixing carbon via the rTCA (Hügler et al. 2005, [79]).

### Sulfate reduction in the brine at nearly saturated MgCl<sub>2</sub> concentrations

SR rates reached maximum values of up to  $460 \mu\text{mol kg}^{-1} \text{d}^{-1}$  (Fig. 3g) within the brine at MgCl<sub>2</sub>-equivalent concentrations of  $3.9 \text{ mol kg}^{-1}$  (Fig. 3b). These rates were ~5–20 times higher than the highest rates measured at most other Mediterranean brine basins [17, 49], but about 10 times lower than SR rates at the Bannock brine basin [22]. They were about three orders of magnitude higher than SR rates in brine systems in the Gulf of Mexico [67, 73] or at the Mercator mud volcano in the Gulf of Cadiz [74]. Evidence for potential candidates mediating SR at Kryos derives from our sequencing data and lipid biomarker analyses. In the brine and lower interface, bacterial sequences were mainly related to sulfate reducers typically detected in hypersaline environments (e.g., solar salterns [87] or Mediterranean DHABs [19, 49]): *Desulfovermiculus* of the family *Desulfohalobiaceae* accounted for 25% and 20% of all bacterial sequences in the lower interface and the brine, respectively. Another potential candidate mediating SR in the lower interface and brine is *Desulfobacula* of the *Desulfobacteraceae*, constituting 1% (lower interface) and 3% (brine) of the total bacterial sequences in these layers. Finally, we detected high concentrations of the fatty-acid 10MeC16:0, typical for *Desulfobacteraceae* and possibly originating from this group in these samples [88–91].

Several authors have argued against the possibility of microbial life in the Kryos brine [19, 25, 26]. The argumentation in these contributions was based on biophysical constraints of low water activity and chaotropicity, and on the absence of detectable mRNA of sulfate reducers and methanogenic archaea in the Discovery [25] and the Kryos brines [19]. However, our measurements now provide evidence for an active sulfate-reducing microbial community within the Kryos brine. Our results, together with previous findings of sulfate reduction (and methanogenesis) in the Discovery brine basin [17], thus provide proof for microbial life at a water activity as low as  $0.4 A_w$  [19], in an environment that belongs to the most chaotropic systems on Earth ( $>300 \text{ kJ kg}^{-1}$ ).

### Concluding remarks

Combining geochemical analyses, rate measurements, lipid biomarker, and NGS analyses, we found active (micro-) aerobic methanotrophs, sulfide-oxidizing bacteria (likely using the rTCA pathway for carbon fixation), and sulfate

reducers living in close vicinity at the seawater–brine interface of the Kryos brine basin. Most intriguingly, we measured high sulfate reduction rates at nearly saturated  $\text{MgCl}_2$ -concentrations, providing evidence that microbes can likely be active at a high degree of chaotropy, and very low water activity. The strong stratification of the detected bacterial community suggests that major phyla are autochthonous. Our results substantially broaden the known spectrum of poly-extreme environmental conditions supporting life on Earth and, potentially, beyond [92].

**Acknowledgements** We thank Captain Schneider, the crew and the scientific party of R/V Meteor for the excellent support at sea. Special thanks go to E. van Weerlee, K. Bakker, D. Gallego-Torres, C. Stalder, V. Darakchieva, R. Groenewegen, and to M. L. Goudeau for analytical support. Dagmar Woebken is thanked for help with DNA extraction from glass fiber filters, Kathrin Büttner for assistance with PCR, and Sebastian Miksch for sequence analysis. We also thank the anonymous reviewers for their helpful comments. This work received financial support through a D-A-CH project funded by the Swiss National Science Foundation and the German Research foundation (Grant No. 200021L\_138057, 200020\_159878/1). Further support was provided through the EU COST Action PERGAMON (ESSEM 0902) and the Max Planck Society, Germany.

## Compliance with ethical standards

**Conflict of interest** The authors declare that they have no conflict of interest.

## References

- Capece MC, Clark E, Saleh J, Halford D, Heintz N, Hoskins S, Rothschild LJ. Polyextremophiles and the constraints of terrestrial habitability. In: Seckbach J, Oren A, Stan-Lotter H, editors. *Polyextremophiles. Life under multiple forms of stress*. Dordrecht: Springer; 2013. pp. 3–60.
- Boetius A, Joye SB. Thriving in salt. *Science*. 2009;324:1523–5.
- Stevenson A, Burkhardt J, Cockell CS, Cray JA, Dijksterhuis J, Fox-Powell M, et al. Multiplication of microbes below 0.690 water activity: implications for terrestrial and extraterrestrial life. *Environ Microbiol*. 2015;17:257–77.
- Oren A. Halophilic microbial communities and their environments. *Curr Opin Biotechnol*. 2015;33:119–24.
- Javor B. *Hypersaline environments: microbiology and biogeochemistry*. Berlin: Springer Science & Business Media; 2012.
- Hansen CJ, Esposito L, Stewart AI, Colwell J, Hendrix A, Pryor W, et al. Enceladus' water vapor plume. *Science*. 2006;311:1422–5.
- McEwen AS, Dundas CM, Mattson SS, Toigo AD, Ojha L, Wray JJ, et al. Recurring slope lineae in equatorial regions of Mars. *Nat Geosci*. 2014;7:53–58.
- Martín-Torres FJ, Zorzano M-P, Valentín-Serrano P, Harri A-M, Genzer M, Kempainen O, et al. Transient liquid water and water activity at Gale crater on Mars. *Nat Geosci*. 2015;8:357–61.
- Preston LJ, Dartnell LR. Planetary habitability: lessons learned from terrestrial analogues. *Int J Astrobiol*. 2014;13:81–98.
- Stock A, Filker S, Yakimov M, Stoeck T. Deep hypersaline anoxic basins as model systems for environmental selection of microbial plankton. In: Seckbach J, Oren A, Stan-Lotter H, editors. *Polyextremophiles. Life under multiple forms of stress*. Dordrecht: Springer; 2013. pp. 499–516.
- Hsü KJ, Ryan WBF, Cita MB. Late Miocene desiccation of the Mediterranean. *Nature*. 1973;242:240–4.
- Camerlenghi A. Anoxic basins of the eastern Mediterranean: geological framework. *Mar Chem*. 1990;31:1–19.
- Roveri M, Flecker R, Krijgsman W, Lofi J, Lugli S, Manzi V, et al. The Messinian salinity crisis: past and future of a great challenge for marine sciences. *Mar Geol*. 2014;352:25–58.
- De Lange GJ, Ten Haven HL. Recent sapropel formation in the eastern Mediterranean. *Nature*. 1983;305:797–8.
- Wallmann K, Suess E, Westbrook G, Winckler G, Cita M, The Medriff Consortium. Salty brines on the mediterranean seafloor. *Science*. 1997;387:31–32.
- Vengosh A, de Lange GJ, Starinsky A. Boron isotope and geochemical evidence for the origin of Urania and Bannock brines at the eastern Mediterranean: effect of water-rock interactions. *Geochim Cosmochim Acta*. 1998;62:3221–8.
- van der Wielen PW, Bolhuis H, Borin S, Daffonchio D, Corselli C, Giuliano L, et al. The enigma of prokaryotic life in deep hypersaline anoxic basins. *Science*. 2005;307:121–3.
- La Cono V, Smedile F, Bortoluzzi G, Arcadi E, Maimone G, Messina E, et al. Unveiling microbial life in new deep-sea hypersaline Lake Thetis. Part I: Prokaryotes and environmental settings. *Environ Microbiol*. 2011;13:2250–68.
- Yakimov MM, La Cono V, Spada GL, Bortoluzzi G, Messina E, Smedile F, et al. Microbial community of the deep-sea brine Lake Kryos seawater–brine interface is active below the chaotropy limit of life as revealed by recovery of mRNA. *Environ Microbiol*. 2015;17:364–82.
- De Lange GJ, Catalano G, Klinkhammer GP, Luther GW. The interface between oxic seawater and the anoxic Bannock Brine; its sharpness and the consequences for the redox-related cycling of Mn and Ba. *Mar Chem*. 1990;31:205–17.
- Sass AM, Sass H, Coolen MJ, Cypionka H, Overmann J. Microbial communities in the chemocline of a hypersaline deep-sea basin (Urania basin, Mediterranean Sea). *Appl Environ Microbiol*. 2001;67:5392–402.
- Daffonchio D, Borin S, Brusa T, Brusetti L, van der Wielen PW, Bolhuis H, et al. Stratified prokaryote network in the oxic-anoxic transition of a deep-sea halocline. *Nature*. 2006;440:203–7.
- Yakimov MM, La Cono V, Denaro R, D'Auria G, Decembrini F, Timmis KN, et al. Primary producing prokaryotic communities of brine, interface and seawater above the halocline of deep anoxic lake L'Atalante, Eastern Mediterranean Sea. *ISME J*. 2007;1:743–55.
- Pachiadaki MG, Yakimov MM, LaCono V, Leadbetter E, Edgcomb V. Unveiling microbial activities along the halocline of Thetis, a deep-sea hypersaline anoxic basin. *ISME J*. 2014;8:2478–89.
- Hallsworth JE, Yakimov MM, Golyshin PN, Gillion JL, D'Auria G, de Lima Alves F, et al. Limits of life in  $\text{MgCl}_2$ -containing environments: chaotropy defines the window. *Environ Microbiol*. 2007;9:801–13.
- Oren A. Life in magnesium- and calcium-rich hypersaline environments: salt stress by chaotropic ions. In: Seckbach J, Oren A, Stan-Lotter H, editors. *Polyextremophiles: life under multiple forms of stress*. Dordrecht: Springer; 2013. pp. 215–32.
- Litchfield CD. Survival strategies for microorganisms in hypersaline environments and their relevance to life on early Mars. *Meteorit Planet Sci*. 1998;33:813–9.
- Grant WD. Life at low water activity. *Philos Trans R Soc B*. 2004;359:1249–67. <https://doi.org/10.1098/rstb.2004.1502>

29. Wallmann K, Aghib FS, Castradori D, Cita MB, Suess E, Greinert J, Rickert D. Sedimentation and formation of secondary minerals in the hypersaline Discovery Basin, eastern Mediterranean. *Mar Geol.* 2002;186:9–28.
30. Niemann H, Steinle LI, Bles J, Krause S, Bussmann I, Treude T, et al. Toxic effects of butyl elastomers on aerobic methane oxidation. *Limnol Oceanogr.* 2015;13:40–52.
31. Treude T, Boetius A, Knittel K, Wallmann K, Jørgensen BB. Anaerobic oxidation of methane above gas hydrates at Hydrate Ridge, NE Pacific Ocean. *Mar Ecol.* 2003;264:1–14.
32. Jørgensen BB. The sulfur cycle of a coastal marine sediment (Limfjorden, Denmark). *Limnol Oceanogr.* 1977;22:814–32.
33. Steinle L, Schmidt M, Bryant L, Haeckel M, Linke P, Sommer S, et al. Linked sediment and water-column methanotrophy at a man-made gas blowout in the North Sea: Implications for methane budgeting in seasonally stratified shallow seas. *Limnol Oceanogr.* 2016;61:S367–86. <https://doi.org/10.1002/lno.10388>
34. Kallmeyer J, Ferdelman TG, Weber A, Fossing H, Jørgensen BB. A cold chromium distillation procedure for radiolabeled sulfide applied to sulfate reduction measurements. *Limnol Oceanogr.* 2004;2:171–80.
35. Steinle L, Maltby L, Engbersen N, Zopfi J, Bange HW, Lehmann MF, et al. Effects of low oxygen concentrations on aerobic methane oxidation in seasonally hypoxic coastal waters. *Biogeosciences.* 2017;14:1631–45.
36. Bles J, Niemann H, Wenk CB, Zopfi J, Schubert CJ, Jenzer JS, et al. Bacterial methanotrophs drive the formation of a seasonal anoxic benthic nepheloid layer in an alpine lake. *Limnol Oceanogr.* 2014;59:1410–20.
37. Grasshoff K, Kremling K, Ehrhardt M. *Methods of seawater analysis.* Weinheim: Wiley-VCH; 1999.
38. Elvert M, Boetius A, Knittel K, Jørgensen BB. Characterization of specific membrane fatty acids as chemotaxonomic markers for sulfate-reducing bacteria involved in anaerobic oxidation of methane. *Geomicrobiol J.* 2003;20:403–19.
39. Niemann H, Elvert M, Hovland M, Orcutt B, Judd A, Suck I, et al. Methane emission and consumption at a North Sea gas seep (Tommeliten area). *Biogeosciences.* 2005;2:335–51.
40. Moss CW, Lambert-Fair MA. Location of double bonds in monounsaturated fatty acids of *Campylobacter cryaerophila* with dimethyl disulfide derivatives and combined gas chromatography-mass spectrometry. *J Clin Microbiol.* 1989;27:1467.
41. Nichols PD, Guckert JB, White DC. Determination of monounsaturated fatty-acid double-bond position and geometry for microbial monocultures and complex consortia by capillary GC-MS of their dimethyl disulfide adducts. *J Microbiol Meth.* 1986;5:49–55.
42. Woebken D, Teeling H, Wecker P, Dumitriu A, Kostadinov I, DeLong EF, et al. Fosmids of novel marine Planctomycetes from the Namibian and Oregon coast upwelling systems and their cross-comparison with planctomycete genomes. *ISME J.* 2007;1:419–35.
43. Herlemann DPR, Labrenz M, Jurgens K, Bertilsson S, Waniek JJ, Andersson AF. Transitions in bacterial communities along the 2000 km salinity gradient of the Baltic Sea. *ISME J.* 2011;5:1571–9.
44. Gantner S, Andersson AF, Alonso-Sáez L, Bertilsson S. Novel primers for 16S rRNA-based archaeal community analyses in environmental samples. *J Microbiol Methods.* 2011;84:12–8.
45. Schloss PD, Westcott SL, Ryabin T, Hall JR, Hartmann M, Hollister EB, et al. Introducing mothur: open-source, platform-independent, community-supported software for describing and comparing microbial communities. *Appl Environ Microbiol.* 2009;75:7537–41.
46. Quast C, Pruesse E, Yilmaz P, Gerken J, Schweer T, Yarza P, et al. The SILVA ribosomal RNA gene database project: improved data processing and web-based tools. *Nucleic Acids Res.* 2013;41:D590–6.
47. Pitzer KS. Ion interaction approach: theory and data correlation. In: Pitzer KS, editor. *Activity coefficients in electrolyte solutions.* Boca Raton: CRC Press; 1991. pp. 75–153.
48. Samapundo S, Deschuyffeleer N, Van Laere D, De Leyn I, Devlieghere F. Effect of NaCl reduction and replacement on the growth of fungi important to the spoilage of bread. *Food Microbiol.* 2010;27:749–56. <https://doi.org/10.1016/j.fm.2010.03.009>
49. Borin S, Brusetti L, Mapelli F, D'Auria G, Brusa T, Marzorati M, et al. Sulfur cycling and methanogenesis primarily drive microbial colonization of the highly sulfidic Urania deep hypersaline basin. *Proc Natl Acad Sci USA.* 2009;106:9151–6.
50. Mwirichia R, Alam I, Rashid M, Vinu M, Ba-Alawi W, Kamau AA, Ngugi DK, Göker M, Klenk H-P, Bajic V, Stingl U. Metabolic traits of an uncultured archaeal lineage -MSBL1- from brine pools of the Red Sea. *Sci Rep.* 2016;6:19181 <https://doi.org/10.1038/srep19181>.
51. Könneke M, Bernhard AE, José R, Walker CB, Waterbury JB, Stahl DA. Isolation of an autotrophic ammonia-oxidizing marine archaeon. *Nature.* 2005;437:543–6.
52. Coolen MJL, Abbas B, Van Bleijswijk J, Hopmans EC, Kuypers MMM, Wakeham SG, et al. Putative ammonia-oxidizing Crenarchaeota in suboxic waters of the Black Sea: a basin-wide ecological study using 16S ribosomal and functional genes and membrane lipids. *Environ Microbiol.* 2007;9:1001–16. <https://doi.org/10.1111/j.1462-2920.2006.01227.x>
53. Ngugi DK, Blom J, Alam I, Rashid M, Alawi W, Zhang G, et al. Comparative genomics reveals adaptations of a halotolerant thaumarchaeon in the interfaces of brine pools in the Red Sea. *ISME J.* 2015;9:396–411.
54. Eder W, Jahnke LL, Schmidt M, Huber R. Microbial diversity of the brine-seawater interface of the Kebrut Deep, Red Sea, studied via 16S rRNA-gene sequences and cultivation methods. *Appl Environ Microbiol.* 2001;67:3077–85.
55. Fish SA, Shepherd TJ, McGenity TJ, Grant WD. Recovery of 16S ribosomal RNA gene fragments from ancient halite. *Nature.* 2002;417:432–6.
56. Edgcomb VP, Pachiadaki MP, Kormas KA, Paraskevi M, Bernhard JM, Leadbetter ER. Microbial activities in sediments below haloclines of thalassohaline and athalassohaline deep-sea brine lakes. *ISME J.* 2016;10:2643–57.
57. Whiticar MJ. Carbon and hydrogen isotope systematics of bacterial formation and oxidation of methane. *Chem Geol.* 1999;161:291–314.
58. Hanson RS, Hanson TE. Methanotrophic bacteria. *Microbiol Rev.* 1996;60:439–71.
59. Hinrichs KU, Hmelo LR, Sylva SP. Molecular fossil record of elevated methane levels in late Pleistocene coastal waters. *Science.* 2003;299:1214–7.
60. Schubert CJ, Coolen MJ, Neretin LN, Schippers A, Abbas B, Durisch-Kaiser E, et al. Aerobic and anaerobic methanotrophs in the Black Sea water column. *Environ Microbiol.* 2006;8:1844–56.
61. Elvert M, Niemann H. Occurrence of unusual steroids and hopanoids derived from aerobic methanotrophs at an active marine mud volcano. *Org Geochem.* 2008;39:167–77.
62. Wakeham SG, Lewis CM, Hopmans EC, Schouten S, Sinninghe Damsté JS. Archaea mediate anaerobic oxidation of methane in deep euxinic waters of the Black Sea. *Geochim Cosmochim Acta.* 2003;67:1359–74.
63. Jakobs G, Rehder G, Jost G, Kießlich K, Labrenz M, Schmale O. Comparative studies of pelagic microbial methane oxidation within the redox zones of the Gotland Deep and Landsort Deep (central Baltic Sea). *Biogeosciences.* 2013;10:7863–75.

64. Rudd JW, Furutani A, Flett RJ, Hamilton RD. Factors controlling methane oxidation in shield lakes: the role of nitrogen fixation and oxygen concentration. *Limnol Oceanogr.* 1976;21:357–64.
65. Blees J, Niemann H, Wenk CB, Zopfi J, Schubert CJ, Kirf MK, et al. Micro-aerobic bacterial methane oxidation in the chemocline and anoxic water column of deep south-Alpine Lake Lugano (Switzerland). *Limnol Oceanogr.* 2014;59:311–24.
66. Abdallah RZ, Adel M, Ouf A, Sayed A, Ghazy MA, Alam I, et al. Aerobic methanotrophic communities at the Red Sea brine-seawater interface. *Front Microbiol.* 2014;5:487 <https://doi.org/10.3389/fmicb.2014.00487>
67. Wankel SD, Joye SB, Samarkin VA, Shah SR, Friederich G, Melas-Kyriazi J, Girguis PR. New constraints on methane fluxes and rates of anaerobic methane oxidation in a Gulf of Mexico brine pool via in situ mass spectrometry. *Deep Sea Res.* 2010;57:2022–9.
68. Schmidt M, Botz R, Faber E, Schmitt M, Poggenburg J, Garbe-Schönberg D, Stoffers P. High-resolution methane profiles across anoxic brine-seawater boundaries in the Atlantis-II, Discovery, and Kebrut Deeps (Red Sea). *Chem Geol.* 2003;200:359–75.
69. Knittel K, Boetius A. Anaerobic oxidation of methane: progress with an unknown process. *Annu Rev Microbiol.* 2009;63:311–34.
70. Ettwig KF, Shima S, van de Pas-Schoonen KT, Kahnt J, Medema MH, op den Camp HJM, et al. Denitrifying bacteria anaerobically oxidize methane in the absence of Archaea. *Environ Microbiol.* 2008;10:3164–73.
71. Ettwig KF, Zhu B, Speth D, Keltjens JT, Jetten MSM, Kartal B. Archaea catalyze iron-dependent anaerobic oxidation of methane. *Proc Natl Acad Sci USA.* 2016;113:12792–6. <https://doi.org/10.1073/pnas.1609534113>
72. Niemann H, Elvert M. Diagnostic lipid biomarker and stable carbon isotope signatures of microbial communities mediating the anaerobic oxidation of methane with sulfate. *Org Geochem.* 2008;39:1668–77.
73. Joye SB, Samarkin VA, MacDonald IR, Hinrichs K-U, Elvert M, Teske AP, et al. Metabolic variability in seafloor brines revealed by carbon and sulphur dynamics. *Nat Geosci.* 2009;2:349–54.
74. Maignien L, Parkes RJ, Cragg B, Niemann H, Knittel K, Coulon S, et al. Anaerobic oxidation of methane in hypersaline cold seep sediments. *FEMS Microbiol Ecol.* 2013;83:214–31.
75. Koga Y, Morii H. Recent advances in structural research on ether lipids from archaea including comparative and physiological aspects. *Biosci Biotechnol Biochem.* 2005;69:2019–34.
76. Jahnke LL, Orphan VJ, Embaye T, Turk KA, Kubo MD, Summons RE, Des Marais DJ. Lipid biomarker and phylogenetic analyses to reveal archaeal biodiversity and distribution in hypersaline microbial mat and underlying sediment. *Geobiology.* 2008;6:394–410.
77. House CH, Schopf JW, Stetter KO. Carbon isotopic fractionation by Archaeans and other thermophilic prokaryotes. *Org Geochem.* 2003;34:345–56.
78. Bernard BB, Brooks JM, Sackett WM. Light hydrocarbons in recent Texas continental shelf and slope sediments. *J Geophys Res Oceans.* 1978;83:4053–61.
79. Hüglér M, Sievert SM. Beyond the Calvin cycle: autotrophic carbon fixation in the ocean. *Annu Rev Mar Sci.* 2011;3:261–89.
80. Berg IA, Kochelkorn D, Ramos-Vera WH, Say RF, Zarzycki J, Hüglér M, et al. Autotrophic carbon fixation in archaea. *Nat Rev Microbiol.* 2010;8:447–60.
81. Mook WG, Bommerson JC, Staverman WH. Carbon isotope fractionation between dissolved bicarbonate and gaseous carbon dioxide. *Earth Plan Sci Lett.* 1974;22:169–76.
82. Hayes JM. Fractionation of carbon and hydrogen isotopes in biosynthetic processes. *Stable Isot Geochem.* 2001;43:225–77.
83. Monson KD, Hayes JM. Carbon isotopic fractionation in the biosynthesis of bacterial fatty acids. Ozonolysis of unsaturated fatty acids as a means of determining the intramolecular distribution of carbon isotopes. *Geochim Cosmochim Acta.* 1982;46:139–49.
84. Sakata S, Hayes JM, Rohmer M, Hooper AB, Seemann M. Stable carbon-isotopic compositions of lipids isolated from the ammonia-oxidizing chemoautotroph *Nitrosomonas europaea*. *Org Geochem.* 2008;39:1725–34. <https://doi.org/10.1016/j.orggeochem.2008.08.005>
85. Kaneda T. Iso- and anteiso-fatty acids in bacteria: biosynthesis, function, and taxonomic significance. *Microbiol Rev.* 1991;55:288–302.
86. Peters K, Walters C, Moldowan J. The biomarker guide: biomarkers and isotopes in the environment and human history. Cambridge: Cambridge University Press; 2007.
87. Dillon JG, Carlin M, Gutierrez A, Nguyen V, McLain N. Patterns of microbial diversity along a salinity gradient in the Guerrero Negro solar saltern, Baja CA Sur, Mexico. *Front Microbiol.* 2013;4:399.
88. Taylor J, Parkes RJ. The cellular fatty acids of the sulfate-reducing bacteria, *Desulfobacter* sp., *Desulfobulbus* sp. and *Desulfovibrio desulfuricans*. *Microbiology.* 1983;129:3303–9.
89. Dowling NJ, Nichols PD, White DC. Phospholipid fatty-acid and infra-red spectroscopic analysis of a sulfate-reducing consortium. *FEMS Microbiol Lett.* 1988;53:325–33.
90. Frostegård A, Tunlid A, Bååth E. Phospholipid fatty-acid composition, biomass, and activity of microbial communities from two soil types experimentally exposed to different heavy metals. *Appl Environ Microbiol.* 1993;59:3605–17.
91. Rütters H, Sass H, Cypionka H, Rullkötter J. Phospholipid analysis as a tool to study complex microbial communities in marine sediments. *J Microbiol Meth.* 2002;48:149–60.
92. Raghoebarsing AA, Pol A, van de Pas-Schoonen KT, Smolders AJP, Ettwig KF, Rijpstra WIC, et al. A microbial consortium couples anaerobic methane oxidation to denitrification. *Nature.* 2006;440:918–21.